

SCIENTIFIC REPORTS

OPEN

Kynurenine aminotransferase activity of Aro8/Aro9 engage tryptophan degradation by producing kynurenic acid in *Saccharomyces cerevisiae*

Kazuto Ohashi¹, Romanas Chaleckis^{2,3}, Masak Takaine^{1,2}, Craig E. Wheelock^{2,3} & Satoshi Yoshida^{1,2}

Kynurenic acid (KA) is a tryptophan (Trp) metabolite that is synthesised in a branch of kynurenine (KYN) pathway. KYN aminotransferase (KAT) catalyses deamination of KYN, yielding KA. Although KA synthesis is evolutionarily conserved from bacteria to humans, the cellular benefits of synthesising KA are unclear. In this study, we constructed a KAT-null yeast mutant defective in KA synthesis to clarify the cellular function of KA. Amino acid sequence analysis and LC/MS quantification of KA revealed that Aro8 and Aro9 are the major KATs. KA was significantly decreased in the *aro8Δ aro9Δ* double mutant. We found that *aro8Δ aro9Δ* cells did not exhibit obvious defects in growth or oxidative stress response when proper amounts of amino acids are supplied in the media. We further found that *aro8Δ aro9Δ* cells were sensitive to excess Trp. The Trp sensitivity was not rescued by addition of KA, suggesting that Trp sensitivity is not due to the loss of KA. In conclusion, we propose that KAT activity is required for detoxification of Trp by converting it to the less toxic KA.

Kynurenic acid (KA) is a tryptophan (Trp) metabolite first identified in dog urine¹. KA is present in several tissues and physiological fluids in humans^{2–8}. KA has been shown to interact with the AMPA receptor, NMDA receptor, GPR35 receptor, AHR nuclear receptor, and sulfotransferases^{9–17}. Although KA is found in unicellular organisms, such as bacteria and yeasts, its cellular function is still unclear.

KA is synthesised by kynurenine (KYN) aminotransferases (KATs), which catalyse irreversible deamination of KYN to KA in a branch of the KYN pathway. The KYN pathway is conserved from bacteria to humans for Trp catabolism and *de novo* synthesis of NAD⁺ (Fig. 1). NAD⁺ is a well-known coenzyme that is involved in many oxidation-reduction reactions. NAD⁺ is also a substrate in several reactions, including mono- and poly-ADP-ribosylation, cyclic ADP-ribose synthesis, and histone deacetylation^{18–20}. NAD⁺ is synthesised not only via the KYN pathway but also via the salvage of NAD⁺ precursors, which are well-known vitamins such as nicotinic acid (NA) and nicotinamide. Also, nicotinamide ribose, nicotinamide mononucleotide, nicotinic acid ribose, and quinolinic acid have been identified as NAD⁺ precursors^{21–27}. These NAD⁺ precursors are imported into the yeast cells from the media and are assimilated for the NAD⁺ supply^{28,29}. On the other hand, Trp is also utilized for NAD⁺ supply via the KYN pathway. The first step in the pathway is catalysed by Bna2, which converts Trp to formylkynurenine²⁶. The oxidation of formylkynurenine is catalysed by Bna7 to produce KYN³⁰. KYN is then converted either to (i) 3-hydroxykynurenine (3-HK) by Bna4, (ii) anthranilic acid (Ant) by Bna5, or (iii) KA by KAT²⁶. Thus, KYN is at a branch point of this pathway. 3-HK results in NAD⁺ through 3-hydroxyanthranilic acid (3-HA) (Fig. 1)^{26,31}. However, the fate of KA is not known in *S. cerevisiae* or higher eukaryotes, although the degradation pathway was suggested in gram-negative bacterium *Pseudomonas fluorescens*³².

¹Institute for Molecular and Cellular Regulation, Gunma University, Gunma, Japan. ²Gunma University Initiative for Advanced Research (GIAR), Gunma University, Gunma, Japan. ³Division of Physiological Chemistry 2, Department of Medical Biochemistry and Biophysics, Karolinska Institutet, Stockholm, Sweden. Correspondence and requests for materials should be addressed to K.O. (email: ohashi@gunma-u.ac.jp)

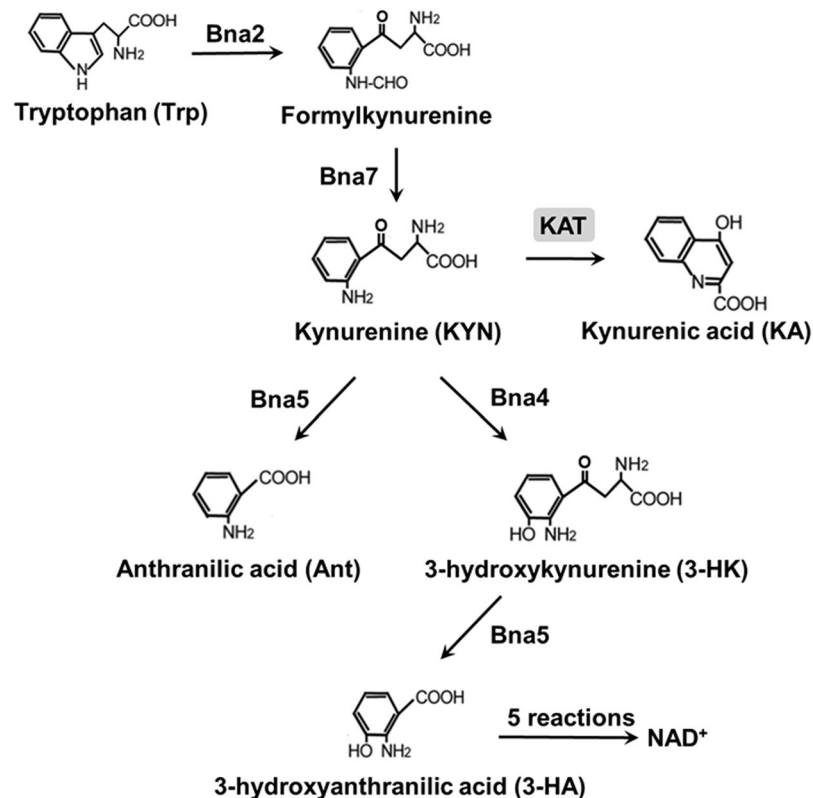


Figure 1. KYN pathway. KYN is synthesised from Trp by Bna2 and Bna7. Bna4, Bna5, and KAT convert KYN to Ant, 3-HK, and KA respectively.

In this study, we confirmed Aro8 and Aro9 as primary KATs in *S. cerevisiae* and showed that the *aro8Δ aro9Δ* mutant cells lack KA. Second, we showed that *aro8Δ aro9Δ* cells were sensitive to high concentrations of Trp. While expression of *ARO9* rescued the sensitivity for Trp in the *aro8Δ aro9Δ* double mutant, addition of KA to the medium did not. These data suggested that KAT activity served to degrade Trp to KA, which is relatively less toxic.

Results

KA was not used as a NAD⁺ precursor. NAD⁺ is synthesised via the KYN pathway (Fig. 1). *S. cerevisiae* cells lacking *BNA2* (*bna2Δ* cells) are inviable in the medium without NAD⁺ precursors, such as NA or nicotinamide, because they lack the ability to synthesise NAD⁺^{23,26}. We tested whether KA and KYN serve as NAD⁺ precursors in the yeast. The growth of *bna2Δ* cells in the presence of KA or KYN was examined, and only KYN, but not KA, rescued the growth of *bna2Δ* cells (Supplementary Fig. S1). Thus, KA is unlikely to be used as a NAD⁺ precursor in the yeast.

Identification of KATs in budding yeast. KATs catalyse the transfer of amine residues from KYN to an alpha keto acid and produce KA. KAT activity was reported in *in vitro* assays using cell lysates of *S. cerevisiae*^{33,34}. A previous report suggested that Bna3, Aro8, and Aro9 have KAT activity³⁰. However, it is unclear whether they are the only KATs in the yeast. To identify the enzyme responsible for KA production in the yeast cells, we tried to re-identify the primary KAT *in silico* and *in vivo*. KATs have been extensively studied in mammals. Four KATs, KAT I (glutamine transaminase K/cysteine conjugate beta-lyase I), KAT II (amino adipate aminotransferase), KAT III (cysteine conjugate beta-lyase 2), and KAT IV (glutamic-oxaloacetic transaminase 2/mitochondrial aspartate aminotransferase) have been identified and characterised in humans^{35–38}. We performed a BLASTP^{39,40} search using the amino acid sequences of human KATs (KAT I, KAT II, KAT III, and KAT IV) as a query. When the BLASTP search was conducted with KAT I, KAT II, or KAT III as a query, 6 proteins (Bna3, Aro9, Aro8, Yer152c, Alt1, and Alt2) were detected as common hits (E-value cut-off, 0.01). When a BLASTP search was conducted with KAT IV as the query, 2 aminotransferases (Aat1 and Aat2) were identified (E-value cut-off, 0.01). Sequence analysis and phylogenetic tree analysis revealed that these 8 proteins contain a common motif (Pfam, pf: Aminotran_1_2) and are predicted as aminotransferases. However, it was difficult to determine the substrate specificity for KYN from their sequence analyses (Fig. 2A, Supplementary Fig. S2). To identify KATs in *S. cerevisiae*, therefore, we measured the concentration of KA and KYN in the cell extract from mutant cells with a gene deletion in KAT candidates (*bna3Δ*, *aro8Δ*, *aro9Δ*, *aat1Δ*, *alt1Δ*, *alt2Δ*, and *yer152cΔ*) by LC/MS. KA was reduced only in *aro9Δ* cell extract (Fig. 2B). Since low levels of KA were still detected in *aro9Δ* cells, we further introduced deletion of the KAT candidate genes into the *aro9Δ* mutant. In the phylogenetic tree of *S. cerevisiae* KAT candidates and human KATs, Aro8 and Aro9 were separated into the same branch with human KAT II,

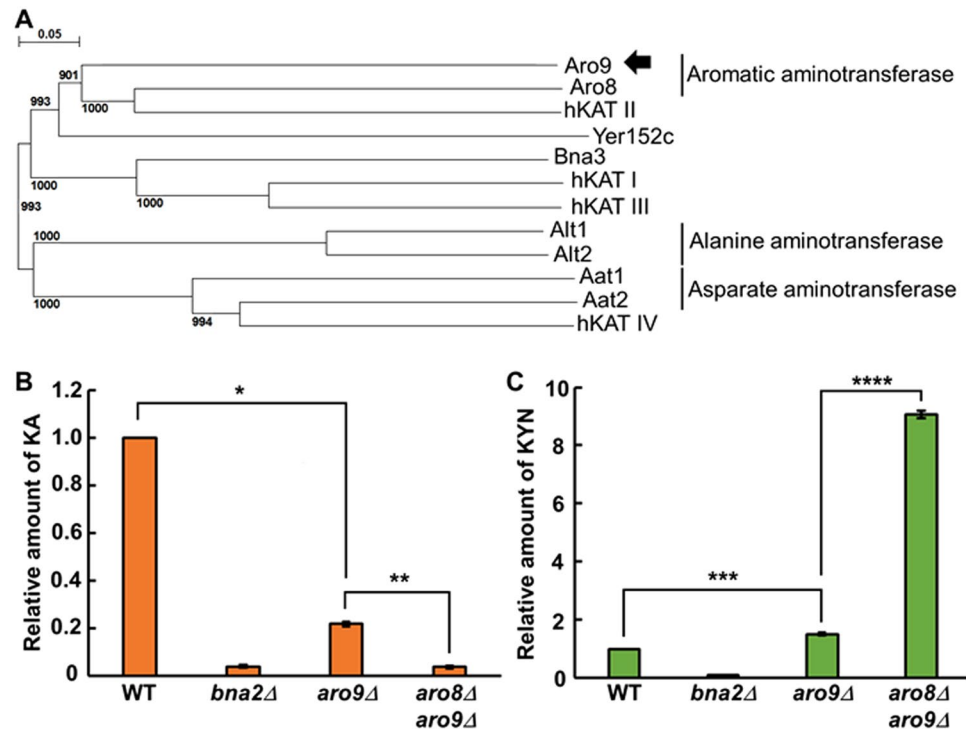


Figure 2. Identification of *S. cerevisiae* KATs for constructing a KA-lacking mutant. **(A)** Phylogenetic tree of *S. cerevisiae* KAT candidates and human KATs. Bootstrap values are indicated on branches. **(B)** LC/MS quantification of intracellular KA levels in the cell extract of the indicated mutants. The values of KA levels are WT: 1, *bna2Δ*: 0.04, *aro9Δ*: 0.22, and *aro8Δ aro9Δ*: 0.04. **(C)** LC/MS quantification of intracellular KYN levels in the cell extract of the indicated mutants. The values of KYN levels are WT: 1, *bna2Δ*: 0.1, *aro9Δ*: 1.5, and *aro8Δ aro9Δ*: 9.1. **(B and C)** Statistical analysis was performed by Welch's *t*-test; **p* = 0.0008, ***p* = 0.0004, ****p* = 0.0009, *****p* = 0.00002. Standard error of the mean is shown by error bars (*n* = 3).

indicating that Aro8 showed the highest similarity to Aro9 (Fig. 2A). Aro9 is 29% identical (51% positively similar amino acids and 13% gaps) to Aro8 and 27% identical (49% positively similar amino acids and 18% gaps) to human KAT II. Therefore, we constructed an *aro8Δ aro9Δ* double mutant and measured the concentration of KA in the cell extract of the mutant. KA was significantly reduced in *aro8Δ aro9Δ* cells to the same level as in *bna2Δ* cells, and KYN was accumulated in *aro8Δ aro9Δ* cells than in *aro9Δ* cells (Fig. 2B,C), indicating that Aro9 and Aro8 are major KATs that produce KA from KYN. The reduction of KA and accumulation of KYN was also confirmed in *aro9Δ* cells (Fig. 2B,C). Notably, KA levels in the *aro8Δ aro9Δ* cells were almost the same as those in *aro8Δ aro9Δ yer152cΔ* and *aro8Δ aro9Δ yer152cΔ bna3Δ* cells, and further reduction of KA was not detected in preliminary data (Supplementary Fig. S3). We also noticed that the levels of KYN are significantly higher in *aro8Δ aro9Δ yer152cΔ* and *aro8Δ aro9Δ yer152cΔ bna3Δ* cells compare with *aro8Δ aro9Δ* cells (Supplementary Fig. S3). The reason why KYN accumulate in *aro8Δ aro9Δ yer152cΔ* and *aro8Δ aro9Δ yer152cΔ bna3Δ* cells remains to be elucidated. We decided to use *aro8Δ aro9Δ* cells as the KA-lacking mutant, although we cannot eliminate the possibility of low amounts of remaining KA. We found that the growth of *aro8Δ aro9Δ* cells was normal on SC media with 30°C incubation (unstressed condition) (Fig. 3A). This suggested that KA is not essential for cell growth.

***aro8Δ aro9Δ* cells were sensitive to high doses of Trp.** To elucidate the cellular function of KA, we investigated *aro8Δ aro9Δ* specific phenotypes. KA was reported to capture radicals and reduce reactive oxygen species^{41–44}. We investigated whether *aro8Δ aro9Δ* cells were sensitive to hydrogen peroxide (H₂O₂). *aro8Δ aro9Δ* cells did not show obvious sensitivity to 3 mM H₂O₂ (Fig. 3A). We also tested several other stresses, including 1 M NaCl, heat shock at 55°C for 50 min, and cold stress at 15°C, but these conditions caused minor growth defects in *aro8Δ aro9Δ* cells (Fig. 3A, Supplementary Fig. S1).

Next, we focused on the role of KAT in the Trp degradation. We investigated whether excess Trp causes a problem in the growth of *aro8Δ aro9Δ* cells. As expected, *aro8Δ aro9Δ* and *aro9Δ* cells showed significant growth defects with 10 mM Trp compared to wild type (WT) cells (Fig. 3B). We confirmed that exogenous expression of Aro9 rescued the growth of *aro8Δ aro9Δ* cells on 4–5 mM Trp (Fig. 3C, Supplementary Fig. S4B). However, the growth deficiency of *aro8Δ aro9Δ* cells by 10 mM Trp was not rescued by adding 10 mM KA (Supplementary Fig. S4A). These data suggested that Aro8 and Aro9 activities, but not KA per se, are responsible for the tolerance to Trp. We observed that the growth of *aro9Δ* and *aro8Δ aro9Δ* cells was much slower than that of *aro8Δ* cells with 10 mM Trp, consistent with our hypothesis that Aro9 is the dominant KAT (Figs 2B and 3B).

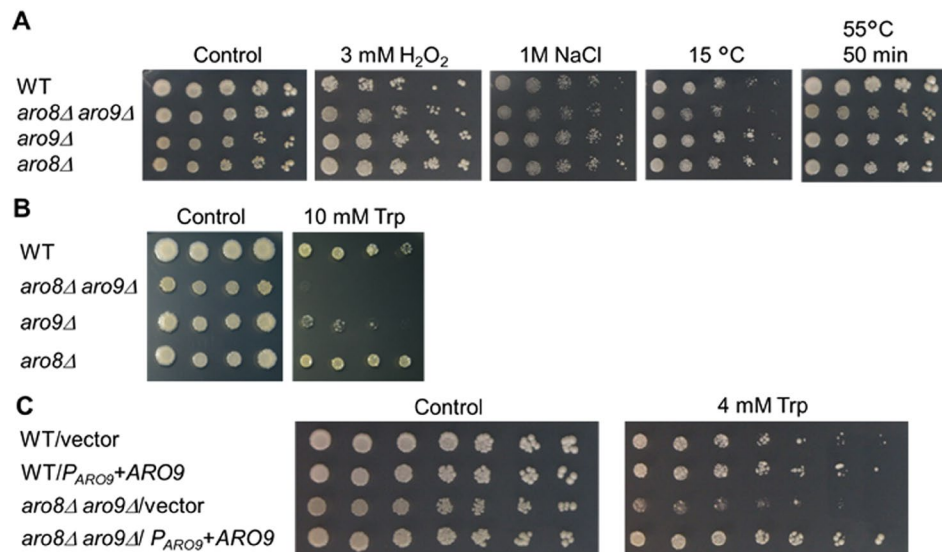


Figure 3. Growth phenotypes of *aro8Δ aro9Δ* cells. SC media with 30 °C incubation was used as an unstressed condition (Control). (A) Growth of *aro8Δ aro9Δ* cells on various stress conditions. The indicated cells were grown for 2–3 days under the stress conditions. (B) Trp sensitivity of *aro8Δ aro9Δ* cells. The indicated cells were grown for 4–5 days in the absence or presence of 10 mM Trp. (C) *ARO9* expression complemented the Trp sensitivity of *aro8Δ aro9Δ* cells. The indicated cells were grown for 4–5 days in the absence or presence of 4 mM Trp.

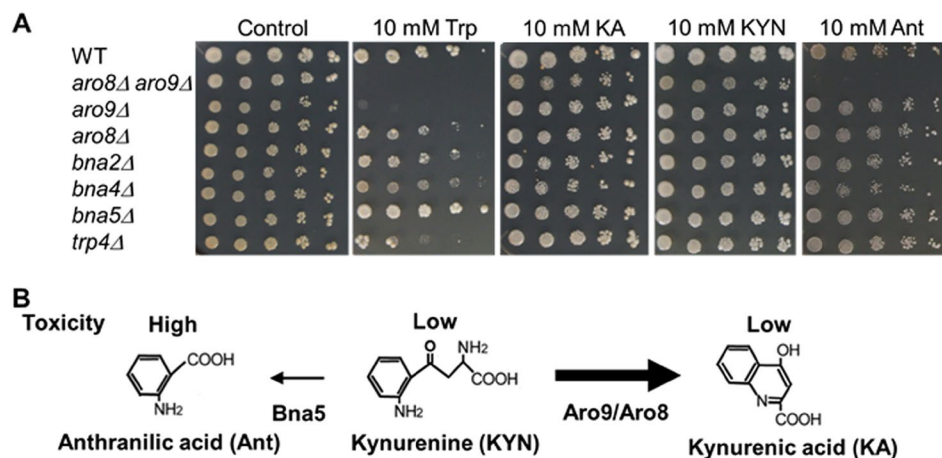


Figure 4. Growth phenotypes of KYN pathway-deficient mutants with high concentration of Trp and its metabolites. (A) Cells with the indicated genotypes were grown for 4–5 days in the absence or presence of 10 mM Trp, 10 mM KA, 10 mM KYN, or 10 mM Ant. (B) Schematic model for detoxification of Trp and Ant by KYN degradation to KA.

Detoxification of Trp and Ant by Aro8 and Aro9. We hypothesised that a metabolite produced downstream of KYN pathway caused the toxic effects in *aro8Δ aro9Δ*. To identify the compound, we examined the growth phenotypes of the KYN pathway mutants on 10 mM Trp medium. *bna2Δ* cells did not show any sensitivity to 10 mM Trp medium (Fig. 4A). However, *bna4Δ* cells were slightly sensitive and *bna5Δ* cells were resistant to 6–10 mM Trp (Fig. 4A, Supplementary Fig. S4C,D). Additionally, we confirmed the accumulation of KYN in *bna4Δ* (Supplementary Fig. S3), which was suggested in a previous report⁴⁵. Because Bna5 is responsible for Ant production from KYN, and Bna4 may reduce toxic Trp metabolites by consumption of KYN, we next examined the toxicity of Ant and KYN. We found that *aro8Δ aro9Δ* was sensitive to 10 mM Ant medium (Fig. 4A). In contrast, none of the mutants were sensitive to KYN or KA (Fig. 4A). These results suggest that toxic metabolites, including Ant, contribute to the toxicity of Trp (Fig. 4B). However, Ant is not the only reason why high dosage of Trp is toxic since Trp toxicity was not attenuated in *bna2Δ* cells defective in Ant synthesis.

Discussion

KA is synthesised by KAT in a branch of the KYN pathway. In humans, four KATs have been identified and characterized^{35–38}. Although KAT activity was biochemically detected in the yeast, it is unclear which gene is

Strains	Descriptions	Resource
WT (BY4741 ^a)	<i>MATa his3-Δ200 leu2-Δ0 ura3-Δ0 met15-Δ0</i>	EUROSCARF
<i>bn2Δ</i>	BY4741 <i>bn2::kanMX4</i>	EUROSCARF
<i>bn4Δ</i>	BY4741 <i>bn4::kanMX4</i>	EUROSCARF
<i>bn5Δ</i>	BY4741 <i>bn5::kanMX4</i>	EUROSCARF
<i>trp4Δ</i>	BY4741 <i>trp4::kanMX4</i>	EUROSCARF
<i>aro8Δ</i>	BY4741 <i>aro8::natNT2</i>	This study
<i>aro8Δ aro9Δ</i>	BY4741 <i>aro8::kanMX4 aro9::hphNT1</i>	This study
<i>aro8Δ aro9Δ yer152cΔ</i>	<i>MATa his3-Δ200 leu2-Δ0 ura3-Δ0 aro8::natNT2 aro9::hphNT1 yer152c::his3MX6</i>	This study
<i>aro8Δ aro9Δ yer152cΔ bn3Δ</i>	BY4741 <i>bn3::kanMX4 aro8::natNT2 aro9::hphNT1 yer152c::his3MX6</i>	This study
<i>bn2Δ bn4Δ</i>	BY4741 <i>bn2::kanMX4 bn4::hphNT1</i>	This study
WT/pSPG1	BY4741 carrying pSPG1	This study
<i>aro8Δ aro9Δ</i> /pSPG1	<i>aro8Δ aro9Δ</i> carrying pSPG1	This study
WT/ <i>P_{ARO9}</i> + ARO9	BY4741 carrying <i>P_{ARO9}</i> + ARO9-pSPG ^b	This study
<i>aro8Δ aro9Δ</i> / <i>P_{ARO9}</i> + ARO9	<i>aro8Δ aro9Δ</i> carrying <i>P_{ARO9}</i> + ARO9-pSPG ^b	This study

Table 1. Yeast strains used in this study. ^aBY4741 was used as WT in this study. ^b2684 bp of DNA from 625 bp upstream to 517 bp downstream of ARO9 ORF was cloned into multi-copy plasmid pSPG1.

responsible for synthesising KA *in vivo*^{26,30,33,34}. In this study, endogenous KA was extracted from cells and quantified by LC/MS. Aro8 and Aro9 were identified as the major enzymes responsible for KA production in the yeast. We showed that *aro8Δ aro9Δ* cells were sensitive to Trp and Ant but not to KA and KYN. In mouse, KYN is believed to be neurotoxic, and KAT in the skeletal muscle protects against neural damage by converting KYN to KA⁴⁶. Similarly, we propose that Aro9 and Aro8 reduce toxic Trp and its metabolites indirectly by converting KYN to KA in the yeast.

Although we focused on KA in this study, Aro8 and Aro9 also catalyse the deamination of Trp to produce indolepyruvate (Supplementary Fig. S5). Notably, Aro9 was reported to prefer Trp to tyrosine or phenylalanine as a substrate^{33,34}. In the detoxification of Trp, Aro9 was more effective than Aro8 (Fig. 3B). Trp aminotransferase activity of Aro9 also should participate in Trp detoxification⁴⁷. Consistent with our proposal that Aro9 is important for the detoxification of Trp, transcription of Aro9 was reported to be induced by Trp^{34,48–50}.

Additionally, we found that *aro8Δ aro9Δ* was sensitive to high concentrations of Ant, although other mutants did not show sensitivity (Fig. 4A). Furthermore, *trp4Δ* cells, which accumulate Ant, were sensitive to Trp, and *bn5Δ* cells, which are defective in Ant synthesis, were resistant to Trp (Fig. 4A). These results identified Ant as one of the potential toxic metabolites produced by excess Trp. However, *trp4Δ* was found to be resistant to Ant (Fig. 4A), suggesting Ant is not the only metabolite that causes toxicity.

In conclusion, we propose that KAT activity primarily contributes to the degradation of excess Trp by converting it to the less toxic KA in the yeast. Given that KA is abundant in urine (in humans, the ratio of KA to KYN is 1.24 in urine⁵¹ and 0.02 in serum⁵²), the role of KAT in detoxification of Trp may be a widely conserved mechanism.

Methods

Yeast cultivations. Standard media, such as yeast extract/peptone/dextrose (YPD) media, were used for the cultivation of *S. cerevisiae*. The optimised minimal medium, which was reported in Hanscho *et al.*⁵³, supplemented with phenylalanine, tyrosine, and Trp was used as SC medium in this study. The detailed composition of 1 L of SC media included 6.7 g yeast nitrogen base (YNB) without amino acid and with ammonium sulfate (Thermo Fisher Scientific, Waltham, USA), 20 g glucose, 0.035 g L-histidine, 0.11 g L-leucine, 0.1 g L-glutamate, 0.12 g L-lysine, 0.04 g L-methionine, 0.1 g L-phenylalanine, 0.38 g L-serine, 0.2 g L-threonine, 0.03 g L-tyrosine, 0.02 g L-Trp, 0.04 g uracil, and 0.006 g inositol. For SC media without Trp and NA, Trp was removed from the composition, and 1.71 g/L YNB without NA (Sunrise Science Products, San Diego, USA) and 5 g/L ammonium sulfate was used instead of YNB. For solid media, 2% agar was added. Additional compounds were sterilised by a 0.2 μm filter and added to the media after autoclaving. Cells were grown aerobically at 30 °C in liquid or solid media. For analysis of the growth phenotype on solid media, 3.0 μl of serially diluted cell suspensions [3-fold serial dilution of cell suspension (A_{600} of 0.2) for Fig. 3B and C and Supplementary Fig. S4B and C, and 5-fold serial dilution of cell suspension (A_{600} of 0.2) for Figs 3A and 4A and Supplementary Figs S1, S4A, and S4D] were spotted onto the SC media containing the indicated compounds and grown at 30 °C under aerobic conditions. An appropriate nutrient was removed from SC media to maintain the plasmid.

Plasmids and strains. A 2684 bp DNA fragment corresponding to the ARO9 ORF flanked by the 625 bp upstream and the 517 bp downstream was amplified by PCR and cloned into SacI/XhoI sites of pSPG1, yielding *P_{ARO9}* + ARO9-pSPG1. Accurate synthesis of all the constructed plasmids was confirmed by DNA sequencing.

Yeast deletion strains (*aro8Δ*, *aro8Δ aro9Δ*, *aro8Δ aro9Δ yer152cΔ*, *aro8Δ aro9Δ yer152cΔ bn3Δ*, and *bn2Δ bn4Δ*) were constructed by PCR-based method using the *his3MX6*, *hphNT1*, or *natNT2* cassette⁵⁴. Correct replacement was confirmed by PCR. Yeast strains used in this study were listed in Table 1.

Extraction of KYN and KA. BY4741 WT, *bna2Δ*, *bna4Δ*, *aro9Δ*, *aro8Δ aro9Δ*, *aro8Δ aro9Δ yer152cΔ*, and *aro8Δ aro9Δ yer152cΔ bna3Δ* cells were diluted to A_{600} of 0.1 in SC media and grown aerobically at 30 °C for 9 h for Fig. 2B and C, and Supplementary Figure S3. Cells were collected following centrifugation ($2,000 \times g$, for 5 min) and quenched by adding pre-cooled ($-20\text{ }^{\circ}\text{C}$) methanol with internal standards. The extraction method was modified for the yeast cells and performed as described⁵⁵.

LC/MS quantification of KYN and KA. Measurement of metabolites by LC/MS was performed using the all ion fragmentation (AIF) method as described in Naz *et al.*⁵⁶. Briefly, yeast cell extracts were measured using an Agilent Ultra-high-performance liquid chromatography (UHPLC) 1290 Infinity II system coupled to a 6550 iFunnel quadrupole-time of flight (Q-TOF) mass spectrometer (Agilent Technologies, Santa Clara, USA). Metabolites were separated using a HILIC SeQuant[®] ZIC[®]-HILIC column (100 mM \times 2.1 mM, 100 Å, 3.5 μm , Merck, Darmstadt, Germany), with a gradient between water [containing 0.1% formic acid (v/v)], and acetonitrile [containing 0.1% formic acid (v/v)]. Database-dependent metabolite screening was performed; the identities of KA and KYN were confirmed by accurate mass, retention time, MS/MS fragments and ion ratios relative to authentic standards. For relative quantification of the KA and KYN, the peak areas of the precursor ions ($[M + H]^+$) were used. Another method described below was used for Supplementary Fig. S3. The LCMS-8050 system (Shimadzu) equipped with a Discovery HS F5-3 Column (2.1 mM \times 150 mM, Sigma-Aldrich) was used. The mobile phase consisted of A [0.1% formic acid (v/v) in water] and B [0.1% formic acid (v/v) in acetonitrile]. Separation was achieved using the appropriate gradient from 100% A (v/v) to 5% A (v/v) and 95% B (v/v). The column was re-equilibrated with 100% A (v/v) for 5 min. The flow rate was 0.25 ml/min. Electrospray ionization was performed in a positive ion mode. Identification of KA and KYN was carried out using standards (KA and KYN from Sigma) with accurate mass, retention time, and MS/MS fragments.

Analysis of the primary structure. For identification of an Aro9 homologue, we used the BLASTP^{39,40} program at KEGG (Kyoto Encyclopedia of Genes and Genomes website, <http://www.genome.jp/kegg/>). Multiple alignment of human KAT II, Aro8, and Aro9 was carried out by ClustalX 2.1⁵⁷. The phylogenetic tree was constructed using the tool for rooted phylogenetic trees with branch length (also by ClustalX 2.1) and drawn by NJprot⁵⁸.

Data availability. The data supporting the findings of this study are included in this article and Supplementary Information.

References

- Liebig, J. Ueber Kynurensäure. *Justus Liebigs Annalen der Chemie* **86**, 125–126 (1853).
- Urbańska, E. M. *et al.* Serum kynurenic acid positively correlates with cardiovascular disease risk factor, homocysteine: a study in stroke patients. *Pharmacol. Rep.* **58**, 507–511 (2006).
- Kuc, D. *et al.* Kynurenic acid in human saliva-does it influence oral microflora? *Pharmacol. Rep.* **58**, 393–398 (2006).
- Parada-Turska, J. *et al.* Kynurenic acid, an endogenous constituent of rheumatoid arthritis synovial fluid, inhibits proliferation of synoviocytes *in vitro*. *Rheumatol. Int.* **26**, 422–426 (2006).
- Hiratsuka, C., Fukuwatari, T. & Shibata, K. Fate of dietary tryptophan in young Japanese women. *Int. J. Tryptophan Res.* **5**, 33–47 (2012).
- Zhao, J. *et al.* Simultaneous determination of urinary tryptophan, tryptophan-related metabolites and creatinine by high performance liquid chromatography with ultraviolet and fluorimetric detection. *J. Chromatogr. B Analyt. Technol. Biomed. Life Sci.* **879**, 2720–2725 (2011).
- Crow, B. *et al.* Analysis of urinary aromatic acids by liquid chromatography tandem mass spectrometry. *Biomed. Chromatogr.* **22**, 1346–1353 (2008).
- Turski, M. P., Turska, M., Paluszkiwicz, P., Parada-Turska, J. & Oxenkrug, G. F. Kynurenic Acid in the digestive system-new facts, new challenges. *Int. J. Tryptophan Res.* **6**, 47–55 (2013).
- Kemp, J. A. *et al.* 7-Chlorokynurenic acid is a selective antagonist at the glycine modulatory site of the N-methyl-D-aspartate receptor complex. *Proc. Natl. Acad. Sci. USA* **85**, 6547–6550 (1988).
- Kessler, M., Terramani, T., Lynch, G. & Baudry, M. A glycine site associated with N-methyl-D-aspartic acid receptors: characterization and identification of a new class of antagonists. *J. Neurochem.* **52**, 1319–1328 (1989).
- Wang, J. *et al.* Kynurenic acid as a ligand for orphan G protein-coupled receptor GPR35. *J. Biol. Chem.* **281**, 22021–22028 (2006).
- Mutz, C. N. *et al.* EWS-FLI1 impairs aryl hydrocarbon receptor activation by blocking tryptophan breakdown via the kynurenine pathway. *FEBS Lett.* **590**, 2063–2075 (2016).
- Lemieux, G. A. *et al.* Kynurenic acid is a nutritional cue that enables behavioral plasticity. *Cell* **160**, 119–131 (2015).
- Olenchock, B. A. *et al.* EGLN1 Inhibition and Rerouting of α -Ketoglutarate Suffice for Remote Ischemic Protection. *Cell* **164**, 884–895 (2016).
- Walczak, K. *et al.* Kynurenic acid synthesis and kynurenine aminotransferases expression in colon derived normal and cancer cells. *Scand. J. Gastroenterol.* **46**, 903–912 (2011).
- Walczak, K. *et al.* Kynurenic acid inhibits proliferation and migration of human glioblastoma T98G cells. *Pharmacol. Rep.* **66**, 130–136 (2014).
- Walczak, K., Turski, W. A. & Rajtar, G. Kynurenic acid inhibits colon cancer proliferation *in vitro*: effects on signaling pathways. *Amino Acids* **46**, 2393–2401 (2014).
- Kim, H., Jacobson, E. L. & Jacobson, M. K. Synthesis and degradation of cyclic ADP-ribose by NAD glycohydrolases. *Science* **261**, 1330–1333 (1993).
- Schreiber, V., Dantzer, F., Ame, J. C. & de Murcia, G. Poly(ADP-ribose): novel functions for an old molecule. *Nat. Rev. Mol. Cell Biol.* **7**, 517–528 (2006).
- Pollak, N., Dölle, C. & Ziegler, M. The power to reduce: pyridine nucleotides-small molecules with a multitude of functions. *Biochem. J.* **402**, 205–218 (2007).
- Belenky, P., Christensen, K. C., Gazzaniga, F., Pletnev, A. A. & Brenner, C. Nicotinamide riboside and nicotinic acid riboside salvage in fungi and mammals. Quantitative basis for Urh1 and purine nucleoside phosphorylase function in NAD⁺ metabolism. *J. Biol. Chem.* **284**, 158–164 (2009).
- Bieganowski, P. & Brenner, C. Discoveries of nicotinamide riboside as a nutrient and conserved NRK genes establish a Preiss-Handler independent route to NAD⁺ in fungi and humans. *Cell* **117**, 495–502 (2004).

23. Ohashi, K., Kawai, S. & Murata, K. Secretion of quinolinic acid, an intermediate in the kynurenine pathway, for utilization in NAD⁺ biosynthesis in the yeast *Saccharomyces cerevisiae*. *Eukaryot. Cell* **12**, 648–653 (2013).
24. Lu, S. P. & Lin, S. J. Phosphate-responsive signaling pathway is a novel component of NAD⁺ metabolism in *Saccharomyces cerevisiae*. *J. Biol. Chem.* **286**, 14271–14281 (2011).
25. Rajavel, M., Lalo, D., Gross, J. W. & Grubmeyer, C. Conversion of a cosubstrate to an inhibitor: phosphorylation mutants of nicotinic acid phosphoribosyltransferase. *Biochemistry* **37**, 4181–4188 (1998).
26. Panozzo, C. *et al.* Aerobic and anaerobic NAD⁺ metabolism in *Saccharomyces cerevisiae*. *FEBS Lett.* **517**, 97–102 (2002).
27. Ghislain, M., Talla, E. & François, J. M. Identification and functional analysis of the *Saccharomyces cerevisiae* nicotinamidase gene, *PNC1*. *Yeast* **19**, 215–224 (2002).
28. Llorente, B. & Dujon, B. Transcriptional regulation of the *Saccharomyces cerevisiae* *DAL5* gene family and identification of the high affinity nicotinic acid permease *TNA1* (YGR260w). *FEBS Lett.* **475**, 237–241 (2000).
29. Belenky, P. A., Moga, T. G. & Brenner, C. *Saccharomyces cerevisiae* *YOR071C* encodes the high affinity nicotinamide riboside transporter *Nrt1*. *J. Biol. Chem.* **283**, 8075–8079 (2008).
30. Wogulis, M., Chew, E. R., Donohoue, P. D. & Wilson, D. K. Identification of formyl kynurenine formamidase and kynurenine aminotransferase from *Saccharomyces cerevisiae* using crystallographic, bioinformatic and biochemical evidence. *Biochemistry* **47**, 1608–1621 (2008).
31. Kucharczyk, R., Zagulski, M., Rytka, J. & Herbert, C. J. The yeast gene *YJR025c* encodes a 3-hydroxyanthranilic acid dioxygenase and is involved in nicotinic acid biosynthesis. *FEBS Lett.* **424**, 127–130 (1998).
32. TANIUCHI, H. & HAYAISHI, O. Studies on the metabolism of kynurenic acid. III. Enzymatic formation of 7,8-dihydroxykynurenic acid from kynurenic acid. *J. Biol. Chem.* **238**, 283–293 (1963).
33. Urrestarazu, A., Vissers, S., Iraqui, I. & Grenson, M. Phenylalanine- and tyrosine-auxotrophic mutants of *Saccharomyces cerevisiae* impaired in transamination. *Mol. Gen. Genet.* **257**, 230–237 (1998).
34. Iraqui, I., Vissers, S., Cartiaux, M. & Urrestarazu, A. Characterisation of *Saccharomyces cerevisiae* *ARO8* and *ARO9* genes encoding aromatic aminotransferases I and II reveals a new aminotransferase subfamily. *Mol. Gen. Genet.* **257**, 238–248 (1998).
35. Han, Q., Robinson, H. & Li, J. Crystal structure of human kynurenine aminotransferase II. *J. Biol. Chem.* **283**, 3567–3573 (2008).
36. Han, Q., Cai, T., Tagle, D. A., Robinson, H. & Li, J. Substrate specificity and structure of human amino adipate aminotransferase/kynurenine aminotransferase II. *Biosci. Rep.* **28**, 205–215 (2008).
37. Han, Q., Robinson, H., Cai, T., Tagle, D. A. & Li, J. Structural insight into the inhibition of human kynurenine aminotransferase I/ glutamine transaminase K. *J. Med. Chem.* **52**, 2786–2793 (2009).
38. Han, Q., Cai, T., Tagle, D. A. & Li, J. Structure, expression, and function of kynurenine aminotransferases in human and rodent brains. *Cell. Mol. Life Sci.* **67**, 353–368 (2010).
39. Altschul, S. F. *et al.* Gapped BLAST and PSI-BLAST: a new generation of protein database search programs. *Nucleic Acids Res.* **25**, 3389–3402 (1997).
40. Schäffer, A. A. *et al.* Improving the accuracy of PSI-BLAST protein database searches with composition-based statistics and other refinements. *Nucleic Acids Res.* **29**, 2994–3005 (2001).
41. Genestet, C. *et al.* Scavenging of reactive oxygen species by tryptophan metabolites helps *Pseudomonas aeruginosa* escape neutrophil killing. *Free Radic. Biol. Med.* **73**, 400–410 (2014).
42. Goda, K., Hamane, Y., Kishimoto, R. & Ogishi, Y. Radical scavenging properties of tryptophan metabolites. Estimation of their radical reactivity. *Adv. Exp. Med. Biol.* **467**, 397–402 (1999).
43. Pérez-González, A., Alvarez-Idaboy, J. R. & Galano, A. Free-radical scavenging by tryptophan and its metabolites through electron transfer based processes. *J. Mol. Model.* **21**, 213 (2015).
44. Zwilling, D. *et al.* Kynurenine 3-monooxygenase inhibition in blood ameliorates neurodegeneration. *Cell* **145**, 863–874 (2011).
45. Giorgini, F., Guidetti, P., Nguyen, Q., Bennett, S. C. & Muchowski, P. J. A genomic screen in yeast implicates kynurenine 3-monooxygenase as a therapeutic target for Huntington disease. *Nat. Genet.* **37**, 526–531 (2005).
46. Agudelo, L. Z. *et al.* Skeletal muscle PGC-1 α 1 modulates kynurenine metabolism and mediates resilience to stress-induced depression. *Cell* **159**, 33–45 (2014).
47. Kradolfer, P., Niederberger, P. & Hütter, R. Tryptophan degradation in *Saccharomyces cerevisiae*: characterization of two aromatic aminotransferases. *Arch. Microbiol.* **133**, 242–248 (1982).
48. Iraqui, I., Vissers, S., André, B. & Urrestarazu, A. Transcriptional induction by aromatic amino acids in *Saccharomyces cerevisiae*. *Mol. Cell. Biol.* **19**, 3360–3371 (1999).
49. Lee, K. & Hahn, J. S. Interplay of Aro80 and GATA activators in regulation of genes for catabolism of aromatic amino acids in *Saccharomyces cerevisiae*. *Mol. Microbiol.* **88**, 1120–1134 (2013).
50. Lee, K., Sung, C., Kim, B. G. & Hahn, J. S. Activation of Aro80 transcription factor by heat-induced aromatic amino acid influx in *Saccharomyces cerevisiae*. *Biochem. Biophys. Res. Commun.* **438**, 43–47 (2013).
51. Bouatra, S. *et al.* The human urine metabolome. *PLoS One* **8**, e73076 (2013).
52. Fukushima, T. *et al.* Quantitative analyses of schizophrenia-associated metabolites in serum: serum D-lactate levels are negatively correlated with gamma-glutamylcysteine in medicated schizophrenia patients. *PLoS One* **9**, e101652 (2014).
53. Hanscho, M. *et al.* Nutritional requirements of the BY series of *Saccharomyces cerevisiae* strains for optimum growth. *FEMS Yeast Res.* **12**, 796–808 (2012).
54. Janke, C. *et al.* A versatile toolbox for PCR-based tagging of yeast genes: new fluorescent proteins, more markers and promoter substitution cassettes. *Yeast* **21**, 947–962 (2004).
55. Kubo, A. *et al.* Semi-quantitative analyses of metabolic systems of human colon cancer metastatic xenografts in livers of superimmunodeficient NOG mice. *Anal. Bioanal. Chem.* **400**, 1895–1904 (2011).
56. Naz, S. *et al.* Development of a Liquid Chromatography-High Resolution Mass Spectrometry Metabolomics Method with High Specificity for Metabolite Identification Using All Ion Fragmentation Acquisition. *Anal. Chem.* **89**, 7933–7942 (2017).
57. Larkin, M. A. *et al.* Clustal W and Clustal X version 2.0. *Bioinformatics* **23**, 2947–2948 (2007).
58. Perrière, G. & Gouy, M. WWW-query: an on-line retrieval system for biological sequence banks. *Biochimie* **78**, 364–369 (1996).

Acknowledgements

This work was supported by a grant from the Japan Foundation for Applied Enzymology (to KO) and start up fund from Gunma University. We thank Touko Hirano (Gunma University, Gunma, Japan) for performing the Shimadzu LC/MS measurements.

Author Contributions

K.O. performed experiments, analysed data, and designed this study. R.C. performed and analysed metabolite measurements. C.E.W. contributed to the identification of metabolites. M.T. and S.Y. contributed to data analysis and study design. All authors participated in writing of the manuscript.

Additional Information

Supplementary information accompanies this paper at <https://doi.org/10.1038/s41598-017-12392-6>.

Competing Interests: The authors declare that they have no competing interests.

Publisher's note: Springer Nature remains neutral with regard to jurisdictional claims in published maps and institutional affiliations.



Open Access This article is licensed under a Creative Commons Attribution 4.0 International License, which permits use, sharing, adaptation, distribution and reproduction in any medium or format, as long as you give appropriate credit to the original author(s) and the source, provide a link to the Creative Commons license, and indicate if changes were made. The images or other third party material in this article are included in the article's Creative Commons license, unless indicated otherwise in a credit line to the material. If material is not included in the article's Creative Commons license and your intended use is not permitted by statutory regulation or exceeds the permitted use, you will need to obtain permission directly from the copyright holder. To view a copy of this license, visit <http://creativecommons.org/licenses/by/4.0/>.

© The Author(s) 2017